

Investigation of Frontal Zones in the Norwegian Sea

A. F. Akhtyamova ✉, V. S. Travkin

St. Petersburg University, Saint Petersburg, Russian Federation

✉ avellinna@gmail.com

Abstract

Purpose. Frontal zones are the areas of strong horizontal gradients of physical, chemical and biological parameters that have a significant impact on the dynamics of the Global Ocean. The aim of the paper is to study the spatial and vertical distribution (including seasonal and interannual variability) of frontal zones in the Norwegian Sea.

Methods and Results. The data on temperature, salinity, sea surface height and velocities from the GLORYS12V1 reanalysis for 1993–2019 available on the CMEMS (Copernicus Marine Environment Monitoring Service) resource, were used. Five mesoscale frontal zones in the area under study were identified, and the average and maximum gradients in the temperature, salinity and sea surface height fields were calculated. The maps of spatial distribution of the thermohaline and dynamic frontal zones, and also of the frequency of frontal zones were constructed. The correlation between the atmospheric indices NAO (North Atlantic Oscillation) and AO (Arctic Oscillation), and the temporal and interannual variability of the frontal zone areas was assessed.

Conclusions. It is shown that the thermohaline and dynamic gradients observed in winter are on the average higher than those observed in summer. It is found that increase of depth is accompanied by a shift of the frontal zones towards the Lofoten Basin and the Faroe-Iceland threshold. The frontal zones frequency maps demonstrate a high rate ($\geq 50\%$) of the areas with strong gradients near the Lofoten Vortex, Svalbard, the Mohn Ridge and the Norwegian continental slope. The majority of frontal zones are of well pronounced seasonal and interannual variability. A negative interannual correlation is noted between the frontal zones areas and the NAO and AO indices. It is also shown that seasonal variability is in high positive correlation with NAO.

Keywords: Norwegian Sea, frontal zones, seasonal variability, interannual variability, NAO index, AO index, arctic oscillation

Acknowledgments: The study was supported financially by the Russian Science Foundation, project No. 22-27-00004.

For citation: Akhtyamova, A.F. and Travkin, V.S., 2023. Investigation of Frontal Zones in the Norwegian Sea. *Physical Oceanography*, 30(1), pp. 62-77. doi:10.29039/1573-160X-2023-1-62-77

DOI: 10.29039/1573-160X-2023-1-62-77

© A. F. Akhtyamova, V. S. Travkin, 2023

© Physical Oceanography, 2023

1. Introduction

The study of water circulation is important both for the development of fundamental knowledge about the nature of the World Ocean and for solving applied problems related to the development of biological and mineral resources of marine areas. Currently, an increasing interest to oceanic fronts for the following reasons is observed: large-scale fronts have a significant impact on weather and climate [1], various marine processes and characteristics, such as high biological productivity [2–6], convection intensity, as well as high velocity of jet streams [7, 8], and others, are associated with fronts.

The phenomenon of frontogenesis has been studied rather poorly; various criteria for selection and terminology are still used. The following definitions were taken as the basis of this study: a front is the result of the intersection of the frontal



interface with any given surface, particularly with the free surface of the ocean or with an isopycnal surface ¹ (Fig. 1). On the other hand, the oceanic front is a relatively narrow zone of enhanced horizontal gradients in physical, chemical, and biological properties (temperature, salinity, nutrients, etc.) that separates wider areas with different vertical structure (stratification) ².

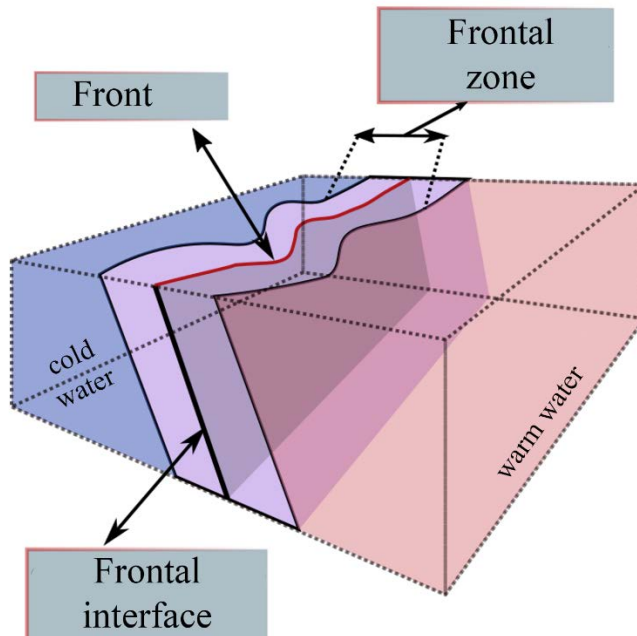


Fig. 1. Structure of the frontal zone in the temperature field

Frontal zones (FZs) are a certain space in which waters of different characteristics interact ¹. The temporal and spatial evolution of fronts is significantly affected by external and internal factors [9]. The external factors include wind action and heat exchange with the atmosphere, the effect of currents, and tidal processes. The internal factors are represented by barotropic and baroclinic flow instability.

The Norwegian Sea is a unique region to study, as it is where the waters of the Atlantic and Arctic Oceans meet, and the associated currents are fundamental to global climate (Fig. 2). The deep part of the Norwegian Sea is represented by two large basins: Norwegian in the southwestern part and Lofoten in the northeastern part, separated by the Vøring Plateau and the Helgeland Ridge (Fig. 2). The Norwegian Basin has a highly rugged relief with numerous

¹ Fedorov, K.N., 1986. *The Physical Nature and Structure of Oceanic Fronts*. Leningrad: Gidrometeoizdat, 296 p. (in Russian); Gruzinov, V.M., 1986. [*Hydrology of Frontal Zones of the World Ocean*]. Leningrad: Gidrometeoizdat, 272 p. (in Russian).

² Fedorov, K.N., 1986. *The Physical Nature and Structure of Oceanic Fronts*. Leningrad: Gidrometeoizdat, 296 p. (in Russian); Belkin, I.M., 2002. Front. In: J. W. Nybakken, 1986. *Interdisciplinary Encyclopedia of Marine Sciences*. Danbury, CT: Grolier Academic Reference. Vol. 1: A-F, pp. 433-435.

seamounts; its maximum depth exceeds 4000 m [10]. In its turn, the Lofoten Basin (LB) is a flat plain bounded by the 3000 m isobath. It is characterized by a local maximum of the ocean surface level, intense heat exchange with the atmosphere, and high energy activity [11–13]. In the center of the LB (at about 69.8°N, 3°E), there is a quasi-permanent intrapycnocline lens, the anticyclonic Lofoten vortex with an average radius of about 37 km [14, 15]. In winter, the deep convection in the LB can exceed 1000 m [16]. The intermediate layer in the central part of the LB is represented by a thick layer of Atlantic waters, which contributes to its transformation into the largest thermal reservoir of the North Atlantic [17, 18].

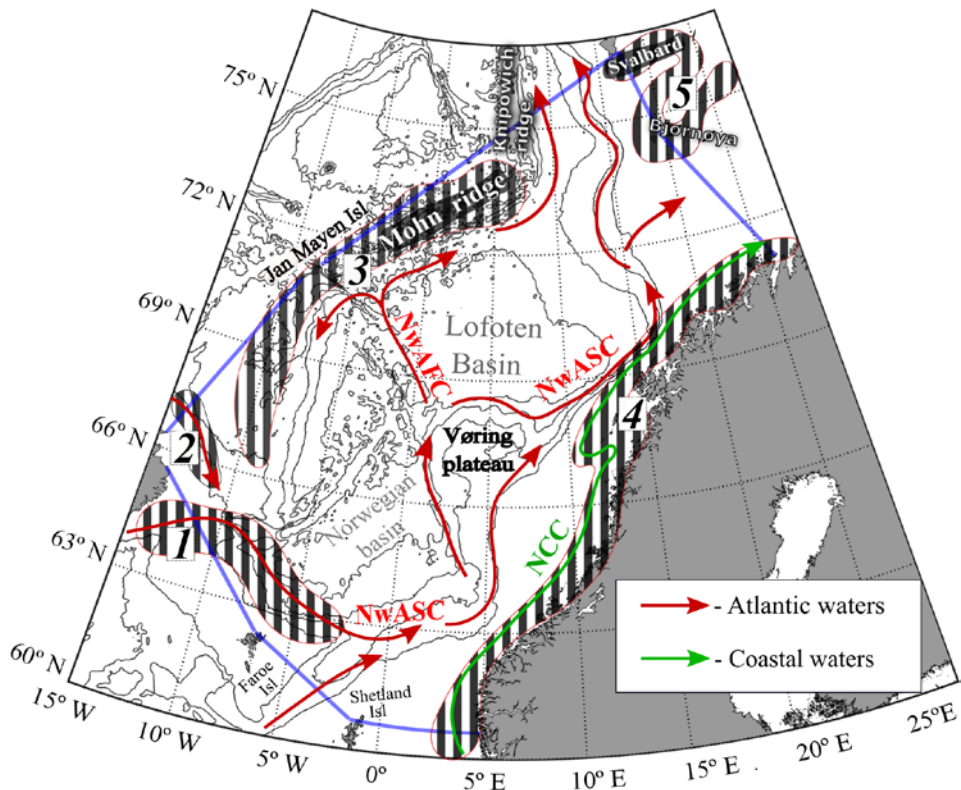


Fig. 2. Map of the area under study. The green color shows the Norwegian Sea boundaries. Frontal zones are shown schematically (shaded areas), numbers denote: 1 – Faroe-Iceland FZ; 2 – East-Iceland Current FZ; 3 – Jan Mayen (Arctic) FZ; 4 – Norwegian Coastal Current FZ; 5 – West Svalbard FZ. Currents: Norwegian Atlantic Slope Current (NwASC), Norwegian Atlantic Frontal Current (NwAFC), Norwegian Coastal Current (NCC) [19, 20]. Isobaths are drawn every 700 m

The Norwegian Current is the northern part of the meridional thermohaline circulation [11]. It consists of two large branches with a pronounced seasonal cycle [21, 22], moving along the boundaries of the LB and carrying the waters of the Atlantic to the north, into the Arctic Basin (Fig. 2). From the west, the LB limits the Norwegian Atlantic Front Current (NwAFC), leaving the Mohn and Knipowich ridges on the left. In the Jan Mayen area, the current is divided into three branches: the first part of it circulates along the western margin of

the Greenland Basin, the second part flows into the Iceland Sea, and the third part, presumably the largest, leaves in a northeasterly direction [23]. From the east, the LB limits the Norwegian Atlantic Slope Current (NwASC). Along the continental slope, the Norwegian Coastal Current (NCC) is located. It is characterized by cold and highly desalinated waters.

A lot of publications are devoted to the study of fronts and FZs of the Norwegian Sea (see the work³ and [24–27]), summarizing which, in the Norwegian Sea, we can distinguish five mesoscale climatic FZs related to the climatic FZ on a planetary scale – the North Polar FZ; the Faroe-Iceland FZ; East Iceland Current FZ; Jan Mayen (Arctic) FZ; Norwegian Coastal Current FZ; West Svalbard FZ (Fig. 2).

Each frontal zone has its own configuration of currents and topography. The study of the Norwegian Sea FZs helps to understand the structure of the climatic large-scale Polar FZ, which is the most important oceanographic feature separating the Atlantic and Arctic waters. It has been determined that the Norwegian Sea FZs state is significantly affected by large-scale atmospheric oscillations, in particular, the North Atlantic Oscillation (NAO) [20]. The essence of the NAO is the redistribution of air masses between the Subtropical Atlantic and the Arctic Basin [28]. The index is calculated as the difference between the normalized surface pressure anomalies between the Azores High and the Icelandic Low. The positive NAO phase contributes to negative sea surface temperature anomalies (SSTA) in the North Atlantic Current and a decrease in the total heat transfer from the ocean to the atmosphere. In its turn, the negative NAO phase is characterized by positive SSTA in the North Atlantic Current, southward displacement of the ice boundary, and increased heat fluxes from the ocean to the atmosphere [29]. A decrease in the NAO index leads to a weakening of the circulation in the Lofoten Basin, which ultimately contributes to the weakening of the Jan Mayen FZ [20].

An index of the Arctic Oscillation (AO) is the main component of the first mode of the empirical orthogonal function (EOF) of mean monthly sea level pressure anomalies in the Northern Hemisphere (20°–90°N) [30]. The AO variability varies from several weeks to decades and has a significant effect on the state of the atmosphere, climate, and sea surface temperature [31]. A close relationship between the AO index and ocean surface temperature [32] has been established. As in the case of the NAO index, the AO index is characterized by a significant correlation with the indicator of surface pressure anomalies in the center of the Azores High and the Icelandic Low. The positive AO phase is characterized by the intensification of polar and subtropical Atlantic air jets and the weakening of the Pacific ones [33]. The negative AO phase contributes to an increase in precipitation in East Asia [32].

Despite the fact that quite a lot of research papers have been devoted to the study of the frontal zones of the Norwegian Sea, unfortunately, there is no clear idea of their spatial structure and interannual variability according to modern data.

³ Korablev, A.A., 1987. [The System of Frontal Sections of the Norwegian EAZO]. In: G. I. Marchuk, ed., 1987. [*Study of the Role of Energy-Active Zones of the Ocean in Short-Term Climate Fluctuations*]. Moscow: VINITI, pp. 380-386 (in Russian).

This paper is an attempt to analyze and quantify the spatiotemporal variability of thermal, haline, and dynamic frontal zones in the Norwegian Sea for 1993–2019, as well as to analyze the relationship between the area of frontal zones and the NAO and AO atmospheric indices.

2. Data

The GLORYS12V1 product used in this paper is a high-quality reanalysis of the global ocean with a daily resolution and a spatial resolution of $1/12^\circ$ at 50 vertical horizons (from 0 to 5500 m). It is based on the CMEMS – a real-time global forecasting system. The oceanic model is NEMO with ECMWF ERA-Interim atmospheric forcing. The observations are assimilated using a reduced-order Kalman filter. The cutout area size is $60^\circ\text{--}77^\circ\text{N}$, $15^\circ\text{W} - 28^\circ\text{E}$.

This work uses data on temperature, salinity, and sea surface height (SSH) for the period from January 1993 to December 2019.

The bathymetry data for the region under study were taken from the ETOPO1 global model of the Earth's surface relief (available at: <https://www.ngdc.noaa.gov>). The model is implemented on a grid with a spatial resolution of $1'$.

3. Processing methods

In order to trace the seasonal variability of the frontal zones, using the MATLAB R2021b program and data on the sea surface height, temperature, and salinity in the Norwegian Sea, the maps of the FZs spatial distribution were constructed. The data processing included several stages:

1. To suppress synoptic variability, three-month averages of temperature, salinity, and sea level over the time period from 1993 to 2019 were extracted from the full array of data. The data were averaged for each season according to the hydrological seasons: winters (January – March), springs (April – June), summer (July – September), and autumn (October – December).

2. The gradients were calculated for each characteristic (temperature, salinity, sea surface height), the average and maximum values of the gradient in the frontal zone were determined. For further calculation, in each detected FZ, the FZ selection condition was applied to the entire calculated data array: for temperature – $|\text{grad } T| \geq 0.02 \text{ }^\circ\text{C}/\text{km}$, for salinity – $|\text{grad } S| \geq 0.01 \text{ psu}/\text{km}$, for sea surface height – $|\text{grad } SSH| \geq 0.002 \text{ m}/\text{km}$.

3. The area of each selected FZ was calculated relative to the geographical space where this FZ is most often manifested.

There are many methods for identifying FZs, including those using altimetry data, as well as satellite images of the microwave, visible, and IR ranges [34–36]. The authors considered the methods for detecting fronts and frontal zones presented in [37–41]. The long-term mean values of temperature and salinity at the nodes of a regular grid, obtained for each season, were used to calculate horizontal gradients according to the algorithm presented in [38]:

$$\frac{\partial P}{\partial x} = \frac{P_{(i,j+1)} - P_{(i,j-1)}}{2S_x}, \quad \frac{\partial P}{\partial y} = \frac{P_{(i+1,j)} - P_{(i-1,j)}}{2S_y},$$

where P is a parameter value in the regular grid node; S_x is a step of the computational grid along the parallel, km, due to the convergence of the meridians to the pole S_x , is not a constant value and is calculated by the formula $S_x = 1,852 \cdot |\lambda_{(i,j+1)} - \lambda_{(i,j)}| \cdot \cos\left(\frac{\varphi_{(i+1,j)} + \varphi_{(i-1,j)}}{2}\right)$; S_y is a computational grid step along the meridian, km, constant value; during the calculations it was determined according to the formula $S_y = 1.852 \cdot |\varphi_{(i+1,j)} - \varphi_{(i,j)}|$, where 1.852 is a length of 1 nautical mile, km; φ and λ are latitude and longitude of grid nodes (deg, min).

Absolute differences $|\lambda_{(i,j+1)} - \lambda_{(i,j)}|$ and $|\varphi_{(i+1,j)} - \varphi_{(i,j)}|$ of the latitude and longitude values between grid points were calculated in geographical minutes and converted to kilometers.

The final module of the horizontal gradient is calculated by the formula

$$|\text{grad } P| = \sqrt{\left(\frac{\partial P}{\partial x}\right)^2 + \left(\frac{\partial P}{\partial y}\right)^2}.$$

This method has an explicit reference to geographic coordinates and helps to compare the gradient values calculated by us and those obtained by other authors, which generally determines the algorithm used as a popular and common choice for processing geodata.

4. Results and discussion

General description of frontal zones

The authors identified and geographically determined five mesoscale FZs in the Norwegian Sea in the field of temperature, salinity, and sea surface height (Fig. 3). The position of the frontal zones is closely related to the bottom topography, as well as to the peculiarity of quasi-stationary current circulation in this region. Based on the analysis results, the following conclusions were made.

For the Faroe-Iceland FZ, the temperature maximum is observed in winter and is 0.20 °C/km, in summer the observed values are half as much and amount to 0.11 °C/km. The average values in the temperature field are 0.034 °C/km while in the work ⁴ they amounted to 0.05 °C/km. Salinity is characterized by a spring maximum – 0.08 psu/km, while in winter the FZ is less pronounced – 0.04 psu/km. The length of the FZ varies from 270 km in summer to 1150 km in winter. This FZ is thermohaline, as it separates warm and saline Atlantic waters from the transformed waters of the central part of the Norwegian Sea ⁵, generating warm and cold eddies, responsible for the main interfrontal exchange of heat, salt, and nutrients [26].

⁴ Korablev, A.A., 1987. [The System of Frontal Sections of the Norwegian EAZO]. In: G. I. Marchuk, ed., 1987. [Study of the Role of Energy-Active Zones of the Ocean in Short-Term Climate Fluctuations]. Moscow: VINITI, pp. 380-386 (in Russian).

⁵ Ibid.

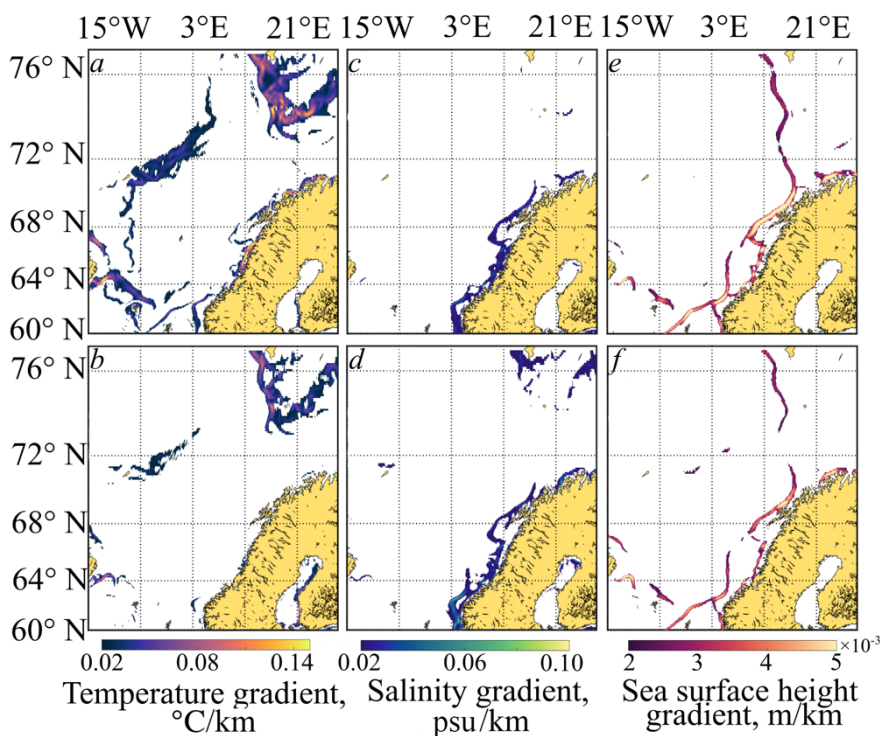


Fig. 3. Gradients of temperature ($^{\circ}\text{C}/\text{km}$) (*a* and *b*), salinity (psu/km) (*c* and *d*) and sea surface height (m/km) (*e* and *f*) averaged over 1993–2019: *on the top* – winter period, *on the bottom* – summer period

The East Iceland Current FZ is not constant. It does not form a haline FZ in the winter, but in summer it manifests itself quite intensively, the maximum gradient is $0.084 \text{ psu}/\text{km}$. The temperature maximum is observed in the autumn and reaches $0.137 \text{ }^{\circ}\text{C}/\text{km}$. The length varies from 170 km in summer to 340 km in winter. In the temperature field, the FZ is more intense in the winter-spring period (average values within the FZ reach $0.039 \text{ }^{\circ}\text{C}/\text{km}$), and in the salinity field – FZ is thermohaline in the spring season ($0.019 \text{ psu}/\text{km}$).

The Jan Mayen (Arctic) FZ is also not constant. The values of salinity gradients are close to zero in winter (there is no FZ), and in summer they reach $0.033 \text{ psu}/\text{km}$, which is a small value relative to other FZs in the region under study. According to A.A. Korablev's work and the paper [42], the gradient in the Arctic FZ is $0.01 \text{ psu}/\text{km}$. This FZ also has the lowest temperature gradients relative to other FZs. The maximum is reached in spring – $0.083 \text{ }^{\circ}\text{C}/\text{km}$, the minimum is reached in summer – $0.056 \text{ }^{\circ}\text{C}/\text{km}$. The obtained average values of the gradients are slightly less than in [20]: $0.03 \text{ }^{\circ}\text{C}/\text{km}$ versus $0.04 \text{ }^{\circ}\text{C}/\text{km}$. The zone is characterized by large spatial dimensions: the length reaches 1380 km, and the average width is 190 km. FZ is mostly thermal, rarely haline. The position of this front in both summer and winter correlates well with the position of the Mohn Ridge. The Arctic front extends from the Iceland-Faroe Plateau to the Mohn and Knipowich ridges [42–45] and is associated with the interaction of warm and saline Atlantic waters with cold and fresher Arctic waters [42–45].

The Norwegian Coastal Current FZ is pronounced in the summer-autumn time in the salinity field due to river runoff, glacier melting, and general circulation. The FZ is related to the change in salinity, which affects the density field in both summer and winter. Here, the maximum salinity gradient is observed in the entire Norwegian Sea and is 0.487 psu/km in autumn, but the FZ is more intense in summer (average values in summer are 0.023 psu/km). In the temperature field, the highest intensity is observed in the autumn and reaches 0.05 °C/km. This FZ is distinguished by its length (up to 2300 km), as it extends along the entire coast of Norway. The width in some areas is also large and reaches 330 km in the salinity field. This FZ is a thermohaline one.

The Western Svalbard FZ is pronounced both in winter and in summer. It meanders strongly and has many fronts. The temperature maximum is observed in spring and reaches 0.25 °C/km. The salinity gradient is more pronounced in summer and is 0.058 psu/km. In winter, the maximum length reaches 1350 km, width – up to 180 km. FZ is also thermohaline. It is caused by the interaction of waters of Atlantic origin with the shelf waters of the Svalbard archipelago penetrating from the Barents Sea [24].

The dynamic frontal zones are largely related to the bottom topography and the location of the cores of the Norwegian Current main branches (Fig. 3, *e* and *f*). Their distribution is very similar to the location of pronounced thermal and haline FZs, for example, the Faroe-Iceland FZ. Seasonal variability is not typical for distinguishing this type of frontal zones and is noticeable only in the Jan Mayen FZ.

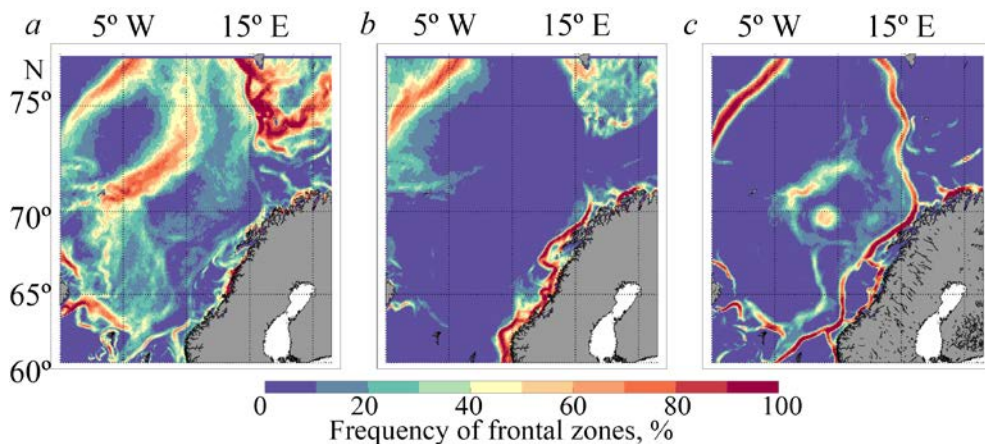


Fig. 4. Frequency of the frontal zones, (%), in the temperature (*a*), salinity (*b*) and sea surface height (*c*) fields over 1993–2019

Fig. 4 demonstrates the FZs frequency in the field of temperature, salinity, and sea surface height for 1993–2019. The West Svalbard FZ is characterized by the highest repeatability in the temperature field (~90–100%) among all FZs. In the salinity field, the Coastal FZ stands out most clearly, since the NCC passes here, carrying significantly desalinated waters, the source of which is a brackish runoff from the Baltic Sea, as well as the runoff from the Norwegian fjords. We see

the opposite picture in the salinity field for the Arctic FZ: the frequency in some places reaches 30% (the FZ is located at a considerable distance from the land). In the level field, a frequency of more than 50% is found in a narrow area of the Norwegian Current cores and in the LB region (Fig. 4, *c*). The Faroe-Iceland FZ can be called the most stable FZ, since it is clearly expressed in all three studied fields. The values found for this FZ are similar to the results obtained using satellite data [34].

When considering the gradients of thermohaline characteristics with increasing depth (Fig. 5), it was found that the depth of occurrence of frontal zones in this water area varies over a wide range. There are both near-surface FZs (located down to the depth of the shelf) and frontal zones covering the entire water column up to the main pycnocline (about 700–1000 m). Large (more than 1000 m) depths of the presence of high gradient zones were not found.

For this water area, with increasing depth, the appearance of other frontal zones that do not occur in the ocean surface layer is typical (for example, the Coastal Slope FZ, which extends along the 500 m isobath, starting from a depth of ~ 300 m, and the Lofoten Vortex FZ), where each FZ is determined by the system of currents, bottom topography, as well as the general interaction of cold and desalinated waters of the Arctic with warm and saline waters of the North Atlantic Current. Nevertheless, the horizon of 50 m is characterized by the largest area of the frontal zones. A transitional boundary of FZ position is the depth of ~ 350 m.

With increasing depth, the frontal zones in the temperature field decrease in size and concentrate closer to the boundaries of the Lofoten Basin (Fig. 5). Two FZs are observed in the salinity field: the frontal zone of the Norwegian Coastal Current, the depth of which reaches approximately 150 m, and the Faroe-Iceland FZ with a characteristic occurrence depth of ~ 250 m (approximately to the depth of the shelf).

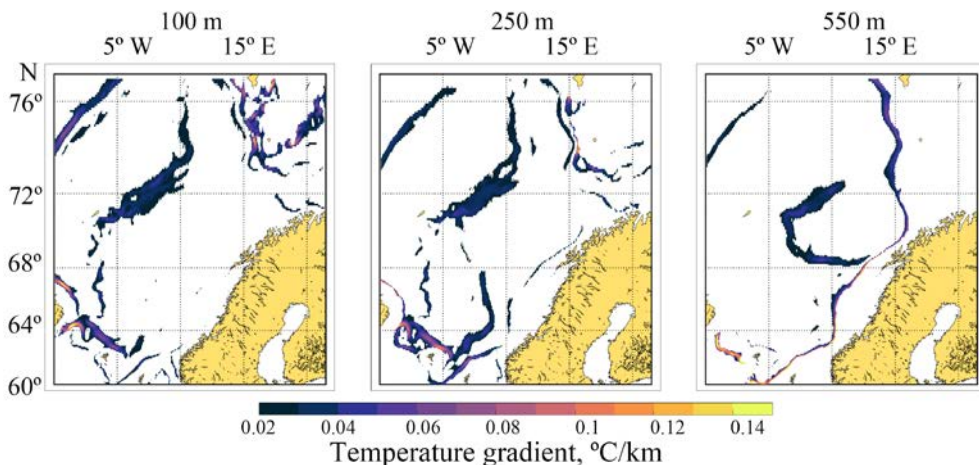


Fig. 5. Spatial distribution of the calculated gradients in the temperature field at the 100, 250 and 550 m depths in 1993–2019

Almost every frontal zone has higher temperature gradients with increasing depth (both maximum and average values). This may be due to intense mixing in the near-surface layer, which cannot be said about the intermediate layer (depths of more than 400 m), in which the warm Norwegian Current meets Arctic waters. Interesting in this regard is the Faroe-Iceland FZ, on the surface of which temperature gradients reach up to $0.13^{\circ}\text{C}/\text{km}$, and at a depth of 550 m they are $0.59^{\circ}\text{C}/\text{km}$.

An analysis of the acquired data revealed that with depth the main role in the FZ dynamics is played by temperature, the gradients of which sharply increase and can be an order of magnitude higher than on the surface. There is a shift of the frontal zones towards the Lofoten Basin and the Faroe-Iceland threshold.

Seasonal and interannual variability

In Fig. 6, *a*, the interannual variability of FZ areas and atmospheric indices are demonstrated. It can be seen that there is a negative interannual correlation between the areas of the Faroe-Iceland and East Iceland FZs with the NAO atmospheric index, equal to -0.44 and -0.51 , respectively (Table). The remaining FZs have a less pronounced negative correlation between the area and NAO. Thus, the correlation values for the Arctic and Coastal FZs, as well as the West Svalbard FZ, are -0.36 , -0.27 , and -0.19 , respectively. The correlation of the area of the studied FZs with the AO index is less pronounced than with the NAO index (Table). It is minimal for the Coastal FZ, while for the West Svalbard FZ it is positive, although is close to zero. For the Arctic, Faroe-Iceland, and East Iceland FZs, the correlation with AO is more pronounced and amounts to -0.27 , -0.32 , and -0.44 , respectively. It should be noted that a significant scatter of correlation values between the investigated FZs is observed. For some FZs, in particular for the West Svalbard and Coastal FZs, the correlation is insignificant both with the NAO index and with the AO index. On the other hand, for the Arctic, Faroe-Iceland, and East Iceland FZs, the correlation values with both the NAO index and the AO index are higher, which may indicate a close relationship between these characteristics of a large-scale atmospheric circulation. The negative interannual correlation between the FZ area and the NAO and AO indices is described in [43] and is associated with the inflow and further distribution of Atlantic waters in the Norwegian Sea.

The Faroe-Iceland and Coastal FZs are characterized by significant negative values of the interannual trend, equal to -988 and $-196\text{ km}^2/\text{year}$ (Table). The East Iceland and Arctic FZs decrease at a slower rate (-86 and $-27\text{ km}^2/\text{year}$, respectively), while the West Svalbard FZ is characterized by a positive interannual trend ($96\text{ km}^2/\text{year}$).

All FZs, except for West Svalbard FZ, are characterized by negative seasonal trends (Table). The highest modulo values of trends are typical for the Faroe-Iceland, Coastal, and Arctic FZs, while for the East-Iceland FZ, the trend is close to zero.

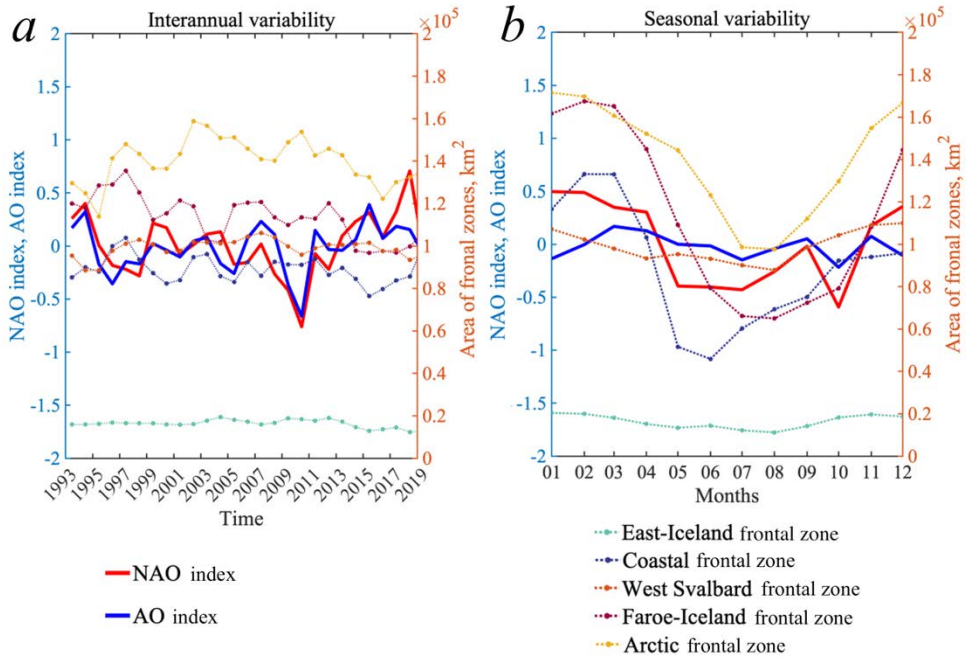


Fig. 6. Interannual and seasonal variability of the frontal zones areas and the NAO and AO indices

Calculated correlations between the FZs areas and the AO and NAO indices, and values of the seasonal and interannual trends

Frontal zones	Correlation				Trends	
	seasonal		interannual		seasonal, km ² /month	interannual, km ² /year
	NAO	AO	NAO	AO		
Faroe-Iceland	0.87	0.33	-0.44	-0.32	-6410.30	-988.41
Arctic	0.78	0.23	-0.36	-0.27	-2691.50	-27.10
East-Iceland	0.66	-0.03	-0.51	-0.44	-118.30	-86.11
Coastal	0.81	0.25	-0.27	-0.05	-3283.75	-196.94
West Svalbard	0.50	-0.18	-0.19	0.14	477.00	96.57

Speaking about seasonal variability (Fig. 6, *b*), it is worth noting that it is typical for the most of FZs and has weak fluctuations only in the East-Iceland FZ and the West Svalbard FZ (Table). In winter, the area of the Arctic and Faroe-Iceland FZs can exceed 160 thousand km², while the area of the Coastal, West Svalbard, and Faroe-Iceland FZs reaches 130, 110, and 20 thousand km², respectively. Most of the FZs reach their maximum spatial development in February, while in spring they sharply decrease. In summer (most often in June or August), the area of the FZ is minimal and for the Arctic, Faroe-Iceland, and Coastal FZs it is 100, 65, and 45 thousand km², respectively (Fig. 6, *b*). The minimum area of the West Svalbard FZ and the East-Iceland FZ in summer reaches 90 and 10 thousand km², respectively. The calculated seasonal variability of the FZ areas is quite similar to the fluctuations in the discharge of the Norwegian Current branches described in [21].

Thus, the area of the Arctic, Faroe-Iceland, and Coastal FZs can change during the year by 1.6, 2.5, and 2.9 times, respectively. In turn, the similar parameters for the West Svalbard FZ and the East-Iceland FZ are 1.2 and 2 times, respectively.

Speaking about the NAO index, we can see that it is maximum in winter and reaches 0.5. Then a sharp decrease in it takes place: by the middle of the spring, it reaches zero, and at the end it reaches -0.4 (Fig. 6). In summer, the NAO index changes slightly, starting to increase only by August. In autumn, a slight increase in the NAO index is noticeable. It is worth noting that in September, there is a significant decrease in both the NAO index and the AO index. Compared to the NAO index, the AO index does not vary so intensively over the seasons (Fig. 6).

5. Conclusions

Based on the GLORYS12V1 reanalysis, the spatial characteristics of the Norwegian Sea FZs were obtained. The estimates of their frequency, seasonal and interannual variability for 1993–2019 are given for the first time. Based on these data, the correlation coefficients of the frontal zones with the NAO and AO indices, as well as the values of the interannual trend, were calculated. The results are largely consistent with the estimates given in earlier studies. Thus, the Jan Mayen and other FZs are clearly traced at depths from 0 to 600 m, which is close to the estimates in other works.

The horizontal temperature gradients in the frontal zones are close to similar estimates in other works, although they may be slightly lower. The gradients in the salinity field have a smaller spread.

The NAO index clearly correlates with the seasonal and interannual variability of the frontal zones, while the relationship with the AO index is less noticeable. Positive values of the correlation between the seasonal variability of the FZ area and the NAO index indicate a decrease in the intensity of frontal zones with a negative NAO index. This mechanism may be related to the displacement of the Norwegian Frontal Current core and the weakening of temperature gradients across the front.

The results indicate a pronounced seasonal and interannual variability of most of the FZs in the Norwegian Sea. In the autumn-winter period, a sharp increase in the area of the frontal zones, which in its values exceeds the long-term changes, takes place. The difference between the area of the frontal zones in summer and

winter can reach 2.5–2.9 times. Most FZs are characterized by negative long-term linear trends, indicating a long-term decrease in their areas. Seasonal and interannual fluctuations of the East-Iceland FZ and West Svalbard FZ are hardly noticeable. The frontal zones are characterized by a pronounced vertical variability from the surface to depths of ~ 900 m. With increasing depth, the position of frontal zones shifts (up to the appearance of new FZs not found on the surface), as well as an increase in temperature and salinity gradients. This fact may be associated with mixing and convection, as well as with the spread of Atlantic waters. It is demonstrated that all FZs have a high frequency (more than 70%) in the temperature field, while in the field of salinity and sea level, the frequency increases only in the region of the Lofoten Vortex and the Norwegian Current cores.

REFERENCES

1. Kostianoy, A.G. and Nihoul, J.C.J., 2009. Frontal Zones in the Norwegian, Greenland, Barents and Bering Seas. In: J. C. J. Nihoul, A. G. Kostianoy, eds., 2009. *Influence of Climate Change on the Changing Arctic and Sub-Arctic Conditions*. Dordrecht: Springer, pp. 171-190. https://doi.org/10.1007/978-1-4020-9460-6_13
2. Olson, D.B., Hitchcock, G.L., Mariano, A.J., Ashjian, C.J., Peng, G., Nero, R.W. and Podestá, G.P., 1994. Life on the Edge: Marine Life and Fronts. *Oceanography*, 7(2), pp. 52-60. <https://doi.org/10.5670/oceanog.1994.03>
3. Bakun, A., 2006. Fronts and Eddies as Key Structures in the Habitat of Marine Fish Larvae: Opportunity, Adaptive Response and Competitive Advantage. *Scientia Marina*, 70(Suppl. 2), pp. 105-122. <https://doi.org/10.3989/scimar.2006.70s2105>
4. Kushnir, V., Pavlov, V., Morozov, A. and Pavlova, O., 2011. “Flashes” of Chlorophyll-a Concentration Derived from in Situ and Remote Sensing Data at the Polar Front in the Barents Sea. *The Open Oceanography Journal*, 5, pp. 14-21. doi:10.2174/1874252101105010014
5. Russell, R.W., Harrison, N.M. and Hunt Jr., G.L., 1999. Foraging at a Front: Hydrography, Zooplankton, and Avian Planktivory in the Northern Bering Sea. *Marine Ecology Progress Series*, 182, pp. 77-93. doi:10.3354/meps182077
6. Mańko, M.K., Merchel, M., Kwasniewski, S. and Weydmann-Zwolicka, A., 2022. Oceanic Fronts Shape Biodiversity of Gelatinous Zooplankton in the European Arctic. *Frontiers in Marine Science*, 9, 941025. doi:10.3389/fmars.2022.941025
7. Chapman, C.C., 2014. Southern Ocean Jets and How to Find Them: Improving and Comparing Common Jet Detection Methods. *Journal of Geophysical Research: Oceans*, 119(7), pp. 4318-4339. doi:10.1002/2014jc009810
8. Orvik, K.A., and Niiler, P., 2002. Major Pathways of Atlantic Water in the Northern North Atlantic and Nordic Seas toward Arctic. *Geophysical Research Letters*, 29(19), 1896. doi:10.1029/2002gl015002
9. Malinin, V.N. and Gordeeva, S.M., 2009. *Fishery Oceanology of South-East Pacific. Volume I. Variability of Habitat Factors*. St. Petersburg: RGGMU Publishing House, 278 p. (in Russian).
10. Belonenko, T.V., Travkin, V.S., Koldunov, A.V. and Volkov, D.L., 2021. Topographic Experiments over Dynamical Processes in the Norwegian Sea. *Russian Journal of Earth Sciences*, 21, ES1006. doi:10.2205/2020ES000747
11. Yu, L.-S., Bosse, A., Fer, I., Orvik, K.A., Bruvik, E.M., Hessevik, I. and Kvalsund, K., 2017. The Lofoten Basin Eddy: Three Years of Evolution as Observed by Seagliders. *Journal of Geophysical Research: Oceans*, 122(8), pp. 6814-6834. doi:10.1002/2017jc012982
12. Bashmachnikov, I.L., Belonenko, T.V. and Kuibin, P.A., 2017. Application of the Theory of Columnar Q-Vortices with Helical Structure for the Lofoten Vortex in the Norwegian Sea.

- Vestnik of St Petersburg University. Earth Sciences*, 62(3), pp. 221-236. doi:10.21638/11701/spbu07.2017.301 (in Russian).
13. Travkin, V.S. and Belonenko, T.V., 2021. Study of the Mechanisms of Vortex Variability in the Lofoten Basin Based on Energy Analysis. *Physical Oceanography*, 28(3), pp. 294-308. doi:10.22449/1573-160X-2021-3-294-308
 14. Raj, R.P., Chafik, L., Nilsen, J.E.Ø., Eldevik, T. and Halo, I., 2015. The Lofoten Vortex of the Nordic Seas. *Deep-Sea Research Part I: Oceanographic Research Papers*, 96, pp. 1-14. doi:10.1016/j.dsr.2014.10.011
 15. Travkin, V.S., Belonenko, T.V. and Kubryakov, A.A., 2022. Cold Spot over the Lofoten Vortex. *Izvestiya, Atmospheric and Oceanic Physics*, 58(12), pp. 1458-1469.
 16. Fedorov, A.M., Bashmachnikov, I.L. and Belonenko, T.V., 2019. Winter Convection in the Lofoten Basin according to ARGO Buoys and Hydrodynamic Modeling. *Vestnik of St Petersburg University. Earth Sciences*, 64(3), pp. 491-511. doi:10.21638/spbu07.2019.308 (in Russian).
 17. Belonenko, T., Zinchenko, V., Gordeeva, S. and Raj, R.P., 2020. Evaluation of Heat and Salt Transports by Mesoscale Eddies in the Lofoten Basin. *Russian Journal of Earth Sciences*, 20, ES6011. doi:10.2205/2020ES000720
 18. Novoselova, E.V. and Belonenko, T.V., 2020. Isopycnal Advection in the Lofoten Basin of the Norwegian Sea. *Fundamental and Applied Hydrophysics*, 13(3), pp. 56-67. doi:10.7868/S2073667320030041 (in Russian).
 19. Volkov, D.L., Kubryakov, A.A. and Lumpkin, R., 2015. Formation and Variability of the Lofoten Basin Vortex in a High-Resolution Ocean Model. *Deep Sea Research Part I: Oceanographic Research Papers*, 105, pp. 142-157. doi:10.1016/j.dsr.2015.09.001
 20. Raj, R.P., Chatterjee, S., Bertino, L., Turiel, A. and Portabella, M., 2019. The Arctic Front and Its Variability in the Norwegian Sea. *Ocean Science*, 15(6), pp. 1729-1744. doi:10.5194/os-15-1729-2019
 21. Mork, K.A. and Skagseth, Ø., 2010. A Quantitative Description of the Norwegian Atlantic Current by Combining Altimetry and Hydrography. *Ocean Science*, 6(4), pp. 901-911. doi:10.5194/os-6-901-2010
 22. Bosse, A. and Fer, I., 2019. Mean Structure and Seasonality of the Norwegian Atlantic Front Current along the Mohn Ridge from Repeated Glider Transects. *Geophysical Research Letters*, 46(22), pp. 13170-13179. doi:10.1029/2019GL084723
 23. Walczowski, W., 2014. *Atlantic Water in the Nordic Seas*. GeoPlanet: Earth and Planetary Sciences. Cham: Springer, 174 p. doi:10.1007/978-3-319-01279-7
 24. Kostianoy, A.G., Nihoul, J.C.J. and Rodionov, V.B., 2004. *Physical Oceanography of Frontal Zones in the Subarctic Seas*. Elsevier, 316 p. doi:10.1016/s0422-9894(04)x8014-4
 25. Johannessen, O.M., 1986. Brief Overview of the Physical Oceanography. In: B. G. Hurdle, ed., 1986. *The Nordic Seas*. New York: Springer, pp. 103-124. doi:10.1007/978-1-4615-8035-5
 26. Belkin, I.M. and Cornillon, P.C., 2007. *Fronts in the World Ocean's Large Marine Ecosystems*. ICES CM 2007/D: 21. International Council for the Exploration of the Sea, 33 p.
 27. Smart, J.H., 1984. Spatial Variability of Major Frontal Systems in the North Atlantic-Norwegian Sea Area: 1980–81. *Journal of Physical Oceanography*, 14(1), pp. 185-192. [https://doi.org/10.1175/1520-0485\(1984\)014<0185:SVOMFS>2.0.CO;2](https://doi.org/10.1175/1520-0485(1984)014<0185:SVOMFS>2.0.CO;2)
 28. Nesterov, E.S., 2013. [*North Atlantic Oscillation: Atmosphere and Ocean*]. Moscow: Triada Ltd, 144 p. (in Russian).
 29. Gulev, S.K., Kolinko, A.V. and Lappo, S.S., 1994. [*Synoptic Interaction of the Ocean and Atmosphere in the Middle Latitudes*]. St. Petersburg: Hydrometeoizdat, 320 p. (in Russian).
 30. Thompson, D.W. and Wallace, J.M., 1998. The Arctic Oscillation Signature in the Wintertime Geopotential Height and Temperature Fields. *Geophysical Research Letters*, 25(9), pp. 1297-1300. doi:10.1029/98GL00950

31. Gong, H., Wang, L., Chen, W. and Nath, D., 2018. Multidecadal Fluctuation of the Wintertime Arctic Oscillation Pattern and Its Implication. *Journal of Climate*, 31(14), pp. 5595-5608. doi:10.1175/jcli-d-17-0530.1
32. Chen, S., Chen, W. and Wu, R., 2015. An Interdecadal Change in the Relationship between Boreal Spring Arctic Oscillation and the East Asian Summer Monsoon around the Early 1970s. *Journal of Climate*, 28(4), pp. 1527-1542. doi:10.1175/JCLI-D-14-00409.1
33. Ambaum, M.H.P., Hoskins, B.J. and Stephenson, D.B., 2001. Arctic Oscillation or North Atlantic Oscillation? *Journal of Climate*, 14(16), pp. 3495-3507. doi:10.1175/1520-0442(2001)014<3495:aoonao>2.0.co;2
34. Belkin, I.M., 2021. Remote Sensing of Ocean Fronts in Marine Ecology and Fisheries. *Remote Sensing*, 13(5), 883. doi:10.3390/rs13050883
35. Miller, P.I., Read, J.F. and Dale, A.C., 2013. Thermal Front Variability along the North Atlantic Current Observed Using Microwave and Infrared Satellite Data. *Deep Sea Research Part II: Topical Studies in Oceanography*, 98(B), pp. 244-256. doi:10.1016/j.dsr2.2013.08.014
36. Wall, C.C., Muller-Karger, F.E., Roffer, M.A., Hu, C., Yao, W. and Luther, M.E., 2008. Satellite Remote Sensing of Surface Oceanic Fronts in Coastal Waters off West-Central Florida. *Remote Sensing of Environment*, 112(6), pp. 2963-2976. doi:10.1016/j.rse.2008.02.007
37. Belkin, I.M. and O'Reilly, J.E., 2009. An Algorithm for Oceanic Front Detection in Chlorophyll and SST Satellite Imagery. *Journal of Marine Systems*, 78(3), pp. 319-326. <https://doi.org/10.1016/j.jmarsys.2008.11.018>
38. Ozhigin, V.K., Ivshin, V.A., Trofimov, A.G., Karsakov, A.L. and Anciferov, M.Y., 2016. *The Barents Sea Water: Structure, Circulation, Variability*. Murmansk: PINRO, 260 p. (in Russian).
39. Moiseev, D.D., Zaporozhtsev, I.F., Maksimovskaya, T.M. and Dukhno, G.N., 2019. Identification of Frontal Zones Position on the Surface of the Barents Sea According to in Situ and Remote Sensing Data. *Arctic: Ecology and Economy*, (2), pp. 48-63. doi:10.25283/2223-4594-2019-2-48-63 (in Russian).
40. Roa-Pascuali, L., Demarcq, H. and Nieblas, A.-E., 2015. Detection of Mesoscale Thermal Fronts from 4km Data Using Smoothing Techniques: Gradient-Based Fronts Classification and Basin Scale Application. *Remote Sensing of Environment*, 164, pp. 225-237. doi:10.1016/j.rse.2015.03.030
41. Foux, V.R., 2009. On Estimation of an Ocean Front Location Depending on the Satellite Measurements. *Fundamental and Applied Hydrophysics*, (1), pp. 29-34 (in Russian).
42. Nilsen, J.E.Ø. and Nilsen, F., 2007. The Atlantic Water Flow along the Vøring Plateau: Detecting Frontal Structures in Oceanic Station Time Series. *Deep Sea Research Part I: Oceanographic Research Papers*, 54(3), pp. 297-319. doi:10.1016/j.dsr.2006.12.012
43. Blindheim, J. and Ådlandsvik, B., 1995. *Episodic Formation of Intermediate Water along the Greenland Sea Arctic Front*. ICES C.M. 1995. Available at: https://www.ices.dk/sites/pub/CM%20Documents/1995/Mini/1995_Mini6.pdf [Accessed: 15 January 2022].
44. Mork, K.A. and Blindheim, J., 2000. Variation in the Atlantic Inflow to the Nordic Seas, 1955-1996. *Deep Sea Research Part I: Oceanographic Research Papers*, 47(6), pp. 1035-1057. doi:10.1016/S0967-0637(99)00091-6
45. Piechura, J. and Walczowski, W., 1995. The Arctic Front: Structure and Dynamics. *Oceanologia*, 37(1), pp. 47-73.

About the authors:

Avelina F. Aktyamova, Engineer-Researcher, Oceanology Department, Saint-Petersburg State University (7–9 Universitetskaya Nab., Saint-Petersburg, Russian Federation, 199034), **ORCID ID: 0000-0001-5447-7654**, avellinnaa@gmail.com

Vladimir S. Travkin, Engineer-Researcher, Oceanology Department, Saint-Petersburg State University (7–9 Universitetskaya Nab., Saint-Petersburg, Russian Federation, 199034), **ORCID ID: 0000-0002-7254-9313**, v.travkin@spbu.ru

Contribution of the co-authors:

Avelina F. Akhtyamova – analysis of literature data, participation in the development of methods, analysis and processing of the obtained data, preparation of graphic material, and the main text of the article.

Vladimir S. Travkin – problem statement, formulation of purposes and objectives of the study, processing of the obtained data, writing and editing the text of the paper

The authors have read and approved the final manuscript.

The authors declare that they have no conflict of interest.